Earthquake Engineering & Structural Dynamics
The Journal of the International Association for Earthquake Engineering

EARTHQUAKE ENGINEERING & STRUCTURAL DYNAMICS
Earthquake Engng Struct. Dyn. 2017
Published online in Wiley Online Library (wileyonlinelibrary.com). DOI: 10.1002/eqe.2915

Dynamics of rocking podium structures

J.A. Bachmann*,†, M.F. Vassiliou and B. Stojadinović

Institute of Structural Engineering (IBK), Swiss Federal Institute of Technology (ETHZ), Stefano-Franscini-Platz 5, 8093 Zurich, Switzerland

SUMMARY

A rocking podium structure is a class of structures consisting of a superstructure placed on top of a rigid slab supported by free-standing columns. The free-standing columns respond to sufficiently strong ground motion excitation by uplifting and rocking. Uplift works as a mechanical fuse that limits the forces transmitted to the superstructure, while rocking enables large lateral displacements. Such 'soft-story' system runs counter to the modern seismic design philosophy but has been used to construct several hundred buildings in countries of the former USSR following Polyakov's rule-of-thumb guidelines: (i) that the superstructure behave as a rigid body and (ii) that the maximum lateral displacement of the rocking podium frame be estimated using elastic earthquake displacement response spectra. The objectives of this paper are to present a dynamic model for analysis of the in-plane seismic response of rocking podium structures and to investigate if Polyakov's rule-of-thumb guidelines are adequate for the design of such structures. Examination of the rocking podium structure response to analytical pulse and recorded ground motion excitations shows that the rocking podium structures are stable and that Polyakov's rule-of-thumb guidelines produce generally conservative designs. Copyright © 2017 John Wiley & Sons, Ltd.

Received 17 February 2017; Revised 7 April 2017; Accepted 15 April 2017

KEY WORDS: rocking structural systems; in-plane seismic response; design guidelines

1. INTRODUCTION

Structures fixed to the ground using foundation systems that prevent uplift and sliding dominate modern seismic design. However, two distinctly different seismic design concepts have emerged over the last half century. One is the concept of seismic base isolation, where an additional soft layer is inserted between the foundation and the superstructure and is specially designed such that it can take most of the seismic displacement demand. Consequently, the seismic demands in the isolated superstructure are decreased, allowing for better-performing and safer structures.

The other concept centers on allowing the structure to uplift from its foundation and rock in response to ground motion excitation. Uplift serves as a mechanical fuse, limiting the forces transmitted to the structure and the foundation, while the energy of the input ground motion is dissipated through impacts at the rocking interfaces. The size effect (larger rocking structures are more stable) and the lack of residual displacements are two remarkable dynamic properties of rocking structures. The pioneering rocking structures have been investigated, designed, and built in New Zealand [1, 2], Russia and the USSR [3], and the USA [4] in 1970s.

Modern rocking buildings evolved in two directions. One direction, developed mainly by North American and New Zealand engineers, focuses on controlling the displacements of rocking buildings using a variety of mechanical restrainers (e.g., post-tensioning cables and yielding bolts) and/or

*Correspondence to: Institute of Structural Engineering (IBK), Swiss Federal Institute of Technology (ETHZ), Stefano-Franscini-Platz 5, 8093 Zurich, Switzerland.
†E-mail: bachmann@ibk.baug.ethz.ch

hysteretic or viscous dampers [5–10]. Another direction, developed mainly in Russia and the USSR, is based on the concept of 'kinematic bearings', where the columns of the entire bottom story of the structures are allowed to rock freely in response to earthquake ground motion excitation, effectively forming a 'flexible story' [11] with the ability to return to its pre-excitation configuration [3]. More than 400 buildings with such 'flexible stories' were built in Russia over the past four decades [12]. The buildings performed well in earthquakes they were exposed to, and the ability of the columns to rock did not deteriorate over the years [12, 13]. Notably, full-scale dynamic tests have been performed on real structures [14, 15]. Figure 1 shows a three-story masonry building placed on a 'kinematic bearing' story being constructed in Russia in 2008. This structure was tested in free rocking motion by applying an initial lateral displacement using hydraulic jacks. The concrete columns of the bottom story of such a rocking structure are designed to uplift and sustain rocking motion during an earthquake event. The ends of the columns are protected by steel plates or caps to avoid concrete crushing when they uplift (Figure 2, left). Insuring that the 'kinematic bearing'

Figure 1. Full-scale dynamic tests of a rocking podium structure [14]: four-story masonry structure (left) and initial displacement of the 'kinematic bearing' story column (right).

Figure 2. Rocking columns in bottom 'kinematic bearing' story: completed and unfinished column [14] (left) and initial displacement of the 'kinematic bearing' story in a free-rocking-motion test [15] (right).

DOI: 10.1002/eqe

story does not collapse (overturn) in a design-basis earthquake and control of the forces in the superstructure is achieved by sizing the rocking columns (Figure 2, right). Design guidelines for such rocking structures were presented in the early 1970s in Polyakov's well-known textbook [3]. He suggested (i) that the superstructure on top of the 'flexible story' behave as a rigid body and (ii) that the dynamics of the 'flexible' first story (the 'kinematic bearing' ground floor) be described using an elastic fixed-base cantilever SDOF model. A similar modeling approach for rocking structures was later suggested by [16].

The study presented in this paper is part of a broad effort undertaken at ETH Zurich to investigate the dynamics of rigid and flexible rocking structures and provide guidelines for their seismic design. A class of rocking podium structures is defined first, followed by the formulation of the equations of rocking motion of such structures. After conducting a dimensional analysis of the equations of motion, they are solved for analytical pulse and recorded ground motion excitation to investigate the stability and maximum deformation demands and capacities of rocking podium structures. The findings indicate that rocking podium structures are stable under earthquake ground motion excitation and that fairly simple design rules of thumb suggested by Polyakov [3] produce conservative designs.

2. ROCKING STRUCTURES

In 1963, Housner [17] proved that out of two geometrically similar blocks, the larger one is more stable when excited dynamically. Accordingly, ground motions with longer dominant periods have a larger overturning potential. In displacement-based design terminology, larger blocks have a larger 'displacement capacity'.

The dynamic behavior of a simple, free-standing rigid rocking block (Figure 3, right) has been systematically studied for more than five decades [18–23]. The behavior of deformable solitary rocking oscillators has also been studied [24–32], to conclude that deformable rocking structures are also remarkably stable when excited by earthquakes. If the ends of the columns are protected, energy dissipation during rocking motion happens instantaneously when the body impacts the ground. Several different modeling approaches have been proposed [33–36] to describe this phenomenon. The probabilistic treatment of the rocking problem [37–39] further confirms the remarkable stability of rocking structures.

In addition to remarkable stability, rocking structures return to their original, undeformed position after the ground motion excitation (if they do not overturn, i.e., collapse), without a residual displacement that inevitably occurs in yielding a fixed-base cantilever structure (Figure 3, left). This dynamic property of rocking structures contributes very significantly to improving their seismic performance for downtime and repair cost performance objectives.

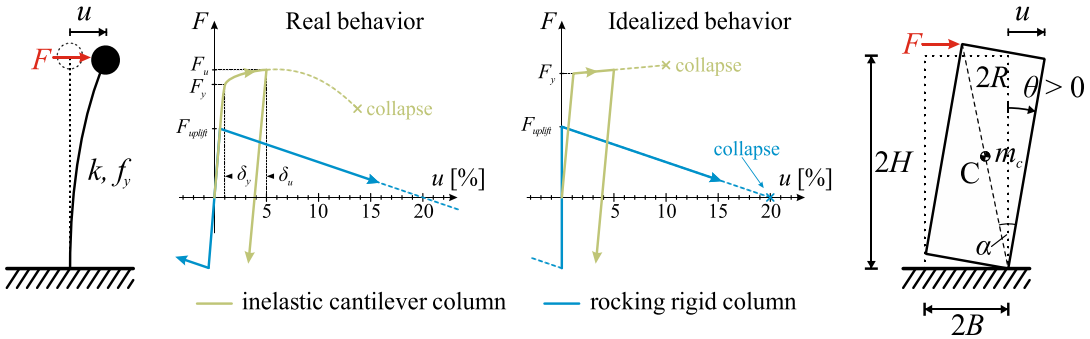

Figure 3. Comparison of force–drift ratio response curves: inelastic cantilever column (left), real and idealized behaviors (middle), and rigid rocking column (right).

DOI: 10.1002/eqe

These favorable dynamic properties, as well as the observation that modern and ancient structures that were unintentionally designed to rock behaved well during earthquakes, have motivated engineers to try to use uplifting and rocking as a structural seismic response modification technique [40–44]. In these structures, uplifting at the interface between rocking structural elements works as a mechanical fuse and limits the forces transmitted to the structure.

The restoring force–displacement behavior for rocking systems idealized as rigid is inherently different from that of a fixed-base SDOF cantilever system (Figure 3, left). Before uplift, the rigid rocking structure does not deform. After uplift, the restoring force in a rocking system decreases as the lateral displacement increases (the system has a negative post-uplift stiffness), while the post-yield resistance of a fixed-base cantilever increases (at least initially, the system has a positive post-yield stiffness). The dynamics of the two systems is very different: Makris and Konstantinidis [45] have shown that approaches based on equivalent elastic SDOF models [16] are not applicable to rocking structures and stated that the elastic response spectra should not be used to evaluate or design rocking structures. The lack of relatively simple rocking structure design models (as opposed to complex response simulation models) continues to deter wider use of rocking structures in earthquake engineering practice.

Rocking frame structures shown in Figure 4 are an important class of rocking structures. They have been proven to be more stable than solitary columns of the same size and slenderness as the columns of the frame [46–50]. Counterintuitively, such rocking frames become more stable as the weight of the cap beam increases [47]. Building [12, 51, 52] and bridge [1] structures based on the rocking frame concept have already been constructed. The objectives of this paper are to present a dynamic model for analysis of the in-plane seismic response of rocking frames that carry a structure (a rocking podium structure, Figure 5) and to investigate if the rule-of-thumb guidelines for seismic design of such structures proposed by Polyakov [3] are adequate.

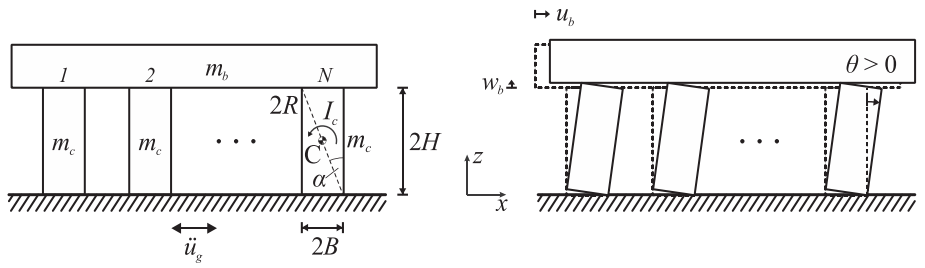

Figure 4. Dynamic model of a rocking frame. Initial position (left) and rocking position (right).

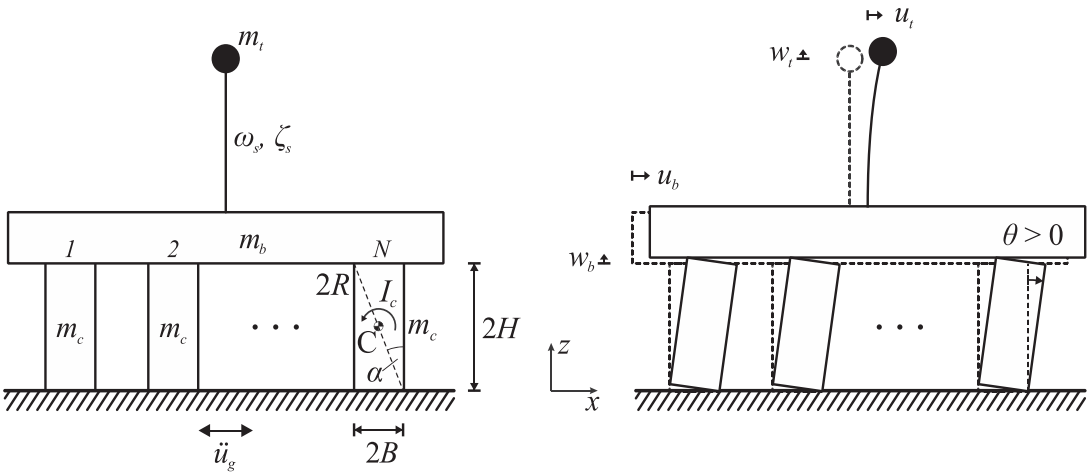

Figure 5. Dynamic model of a rocking podium structure. Initial position (left) and rocking position (right).

DOI: 10.1002/eqe

3. DYNAMIC MODEL OF A ROCKING PODIUM STRUCTURE

The equation of in-plane motion for a rigid rectangular rocking column (Figure 3, right) with slenderness α and a semi-diagonal of length R is

$$\ddot{\theta} = -p^2 \cdot \left(\sin[\pm\alpha - \theta] + \frac{\ddot{u}_g}{g} \cos[\pm\alpha - \theta] \right) \tag{1}$$

where

$$p = \sqrt{(3g)/(4R)} \tag{2}$$

is the frequency parameter of the rocking column. The upper sign in front of α corresponds to a positive, and the lower sign to a negative rocking angle θ with respect to the defined coordinate system (Figure 3, right).

Makris and Vassiliou [46] extended the rocking model of a solitary rigid rectangular column to a rocking frame comprising N rigid columns capped by a rigid beam (Figure 4, left). Uplift of the columns is not restrained, but their sliding on the rocking surface is precluded. The corresponding equation of motion becomes

$$\ddot{\theta} = -\hat{p}^2 \cdot \left(\sin[\pm\alpha - \theta] + \frac{\ddot{u}_g}{g} \cos[\pm\alpha - \theta] \right) \tag{3}$$

where the frequency parameter of the rocking frame is

$$\hat{p} = \sqrt{\frac{1+2\gamma}{1+3\gamma}} \cdot \sqrt{\frac{3g}{4R}} \tag{4}$$

and γ is the mass ratio of the mass of the cap beam divided by the mass of all N columns:

$$\gamma = \frac{m_b}{N m_c} \tag{5}$$

Since the frequency parameter $\hat{p}$ of the rocking frame is always smaller than the frequency parameter of a solitary column p, the response (tilt angle θ) of the rocking frame to the same ground excitation $\ddot{u}_g$ is always smaller than the response of the solitary column. As the mass of the cap beam increases, the mass ratio γ increases and the frequency parameter $\hat{p}$ decreases, leading to a conclusion that rocking frames become more stable as the cap beam becomes more massive.

The response of the rocking frame is equal to the response of an equivalent solitary column that is geometrically similar to, yet larger than, the columns of the frame. The size of the equivalent solitary rocking column is

$$\hat{R} = \frac{1+3\gamma}{1+2\gamma} R \tag{6}$$

Even though most researchers have studied blocks of rectangular solid cross sections, the original derivation by Housner [17] was developed for blocks of general geometry and mass distribution. Therefore, in order to account for rocking frame columns with non-rectangular shapes and/or different mass distributions, in this paper, a mass eccentricity ratio λ is defined as

$$\lambda = \frac{I_C}{m_c R^2} \tag{7}$$

where I_C is the rotational inertia of the column around its center of mass C. Then, the rocking frequency parameter of the rocking frame is equal to

DOI: 10.1002/eqe

$$\widetilde{p} = \sqrt{\frac{1+2\gamma}{1+\lambda+4\gamma}}\sqrt{\frac{g}{R}} \tag{8}$$

and the size of the equivalent solitary column is

$$\widetilde{R} = \frac{1+\lambda+4\gamma}{1+\lambda+2\gamma(1+\lambda)}R \tag{9}$$

The equation of motion of the frame is still given by either Eq. (1) or (3), with the frequency parameter now equal to $\widetilde{p}$.

The value of parameter λ for a solid solitary column with evenly distributed mass and with a uniform rectangular cross section is 1/3. For a column with mass m_c and semi-diagonal R, factor λ could theoretically take values between 0 (mass concentrated in the center of mass C) and 1 (mass distributed at the outside edges of the block). Realistic values for λ are as follows:

- Rectangular column (solid/hollow (thin walled)): λ = 0.33/0.34
- Circular column (solid/hollow (thin walled)): λ = 0.35/0.35
- R/C column with steel end protectors (Figure 2, d_s = 5/10 cm): λ = 0.38/0.40

For example, a rocking frame with common solid rectangular columns (λ = 1/3) of size R, and a very heavy cap beam ($\gamma \to \infty$) the size of the equivalent solitary column $\widetilde{R}$ is 1.50 times larger than the size of the frame column R, matching exactly the value derived in [46].

3.1. Rocking podium structure

A multi-story superstructure built on a rocking first story, akin to the one shown in Figure 2, is modeled as a rocking podium structure shown in Figure 5. The dynamics of the superstructure are assumed to be adequately represented by a SDOF cantilever system. Thus, the rocking frame model described earlier is extended by adding a deformable SDOF system fixed on top of the cap beam of the rocking podium frame. The following assumptions are made:

- The response of the superstructure remains elastic.
- The superstructure mass m_t is lumped at the top and does not have any rotational inertia.
- The overturning moment excreted by the superstructure on the podium cap beam is not large enough to cause uplift of the cap beam (detachment of the beam from the columns).
- The contact surfaces at the bottom and the top of the columns of the rocking podium frame do not allow any sliding and stay intact throughout the rocking motion (there is no crushing or permanent deformation of the contact surfaces).
- The rocking first story is assumed to be rigid.

The rocking podium structure is a two-degree-of-freedom system where the motion of the rocking frame cap beam with respect to the support is described by the displacement u_b (equivalently, tilt angle θ) and the motion of the superstructure mass m_t with respect to the cap beam is described by the displacement u_t. A superstructure mass ratio is defined as

$$\eta = \frac{m_t}{m_b} \tag{10}$$

Assuming that the weight of each story is roughly the same, η can be interpreted as the number of stories above the rocking podium frame.

3.2. Equation of motion before uplift and uplift criterion

The SDOF system representing the multi-story structure on the rocking podium has a fixed-base natural frequency ω_s and a viscous damping ratio ζ_s. Before uplift, the equation of motion of the superstructure on top of the rocking podium frame is

$$\ddot{u}_t + 2\zeta_s\omega_s\dot{u}_t + \omega_s^2 u_t = -\ddot{u}_g \tag{11}$$

DOI: 10.1002/eqe

The rocking podium frame does not move before uplift, removing its degree of freedom from consideration. The uplift criterion for the rocking podium frame with N free-standing columns (each with slenderness α) capped with a rigid beam is the same as for a solitary rigid column of slenderness α:

$$\ddot{u}_{\mathrm{g}} = \pm g \tan \alpha \tag{12}$$

The presence of the superstructure on top of the cap beam modifies this uplift criterion. Figure 6 (right) shows the forces acting on the rocking podium at incipient uplift (for $\theta < 0$). The lateral force V_s is the resulting shear force acting at the base of the SDOF oscillator.

$$V_s = k\,u_t + c\,\dot{u}_t = m_t \cdot \left(\omega_s^2 u_t + 2\zeta_s \omega_s \dot{u}_t\right) \tag{13}$$

The principle of virtual work for a positive $\ddot{u}_g$ and a virtual rotation of $-\delta\theta$ at incipient uplift is applied:

$$\delta\theta \cdot \left(BNm_c g - HNm_c \ddot{u}_g\right) + \delta\theta \cdot (2Bm_b g + 2Bm_t g) - \delta\theta \cdot 2Hm_b \ddot{u}_g + \delta\theta \cdot 2HV_s = 0 \tag{14}$$

Combining Eqs (13) and (14) yields

$$\ddot{u}_g \cdot (2m_b + Nm_c) = g \tan\alpha \cdot (2m_b + 2m_t + Nm_c) + \omega_s^2 m_t u_t + 2\zeta_s \omega_s m_t \dot{u}_t \tag{15}$$

Then, the rocking podium frame uplift thresholds for both positive and negative ground accelerations are

$$\ddot{u}_g = \pm g \tan\alpha + \frac{2\gamma\eta}{2\gamma + 1}\left(\pm g \tan\alpha + \omega_s^2 u_t + 2\zeta_s \omega_s \dot{u}_t\right) \tag{16}$$

For rigid superstructures where $\left(\omega_s^2 u_t + 2\zeta_s \omega_s \dot{u}_t\right) \rightarrow -\ddot{u}_g$ and for light superstructures where $\eta \rightarrow 0$, Eq. (16) resolves to Eq. (12).

3.3. *Equations of motion after uplift*

The Lagrangian formulation is used to derive the equations of motion of the two-degree-of-freedom rocking podium structure after uplift as follows:

$$L = T - V \tag{17}$$

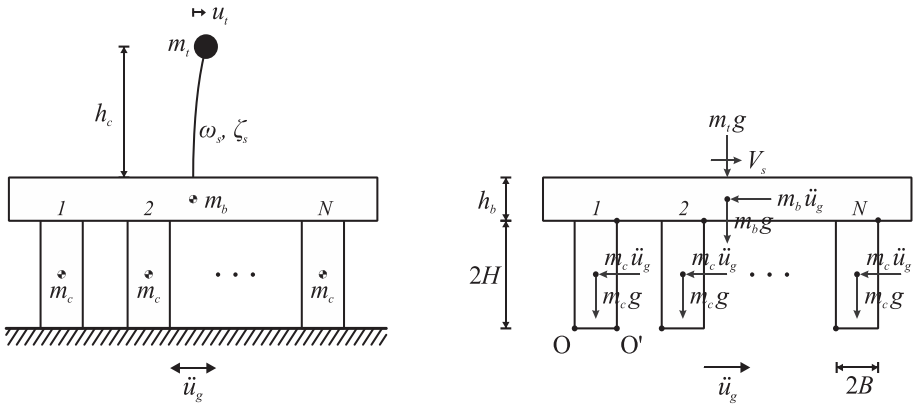

Figure 6. Elastic oscillation of the rocking podium structure due to ground excitation before uplift (left) and internal forces at incipient uplift in response to the ground motion excitation (right).

DOI: 10.1002/eqe

$$\frac{d}{dt}\frac{\partial L}{\partial \dot{q}_i} - \frac{\partial L}{\partial q_i} = Q_{q_i} \tag{18}$$

where T is the kinetic energy stored in the system, V is the potential energy of the system, and Q_{q_i} is the non-conservative force acting along direction q_i, derived from the virtual work W carried out by the forces in the system for a virtual displacement δq_i.

The horizontal displacement and vertical displacement of the rigid cap beam (Figure 5) are

$$\begin{aligned} u_b &= 2R\cdot(\sin[\pm\alpha] - \sin[\pm\alpha - \theta]) \\ w_b &= 2R\cdot(\cos[\pm\alpha - \theta] - \cos\alpha) \end{aligned} \tag{19}$$

The first and second derivatives with respect to time of Eq. (19) are

$$\begin{aligned} \dot{u}_b &= 2R\cdot\dot{\theta}\cos[\pm\alpha - \theta] \\ \ddot{u}_b &= 2R\cdot\left(\ddot{\theta}\cos[\pm\alpha - \theta] + \dot{\theta}^2\sin[\pm\alpha - \theta]\right) \end{aligned} \tag{20}$$

$$\begin{aligned} \dot{w}_b &= 2R\cdot\dot{\theta}\sin[\pm\alpha - \theta] \\ \ddot{w}_b &= 2R\cdot\left(\ddot{\theta}\sin[\pm\alpha - \theta] - \dot{\theta}^2\cos[\pm\alpha - \theta]\right) \end{aligned} \tag{21}$$

The kinetic energy in the system is

$$T = T_t + T_b + T_c = \frac{1}{2}m_t\cdot\left(\dot{u}_t^2 + \dot{w}_t^2\right) + \frac{1}{2}m_b\cdot\left(2R\dot{\theta}\right)^2 + \frac{1}{2}Nm_c\cdot(1+\lambda)\cdot\left(R\dot{\theta}\right)^2 \tag{22}$$

where u_t and w_t are the horizontal and vertical displacement of the top mass. Given that

$$\dot{w}_t = \dot{w}_b \tag{23}$$

Equation (22) yields

$$T = \frac{1}{2}m_t\cdot\left(\dot{u}_t^2 + 4R^2\sin^2[\pm\alpha - \theta]\dot{\theta}^2\right) + \frac{1}{2}m_b\cdot\left(2R\dot{\theta}\right)^2 + \frac{1}{2}Nm_c\cdot(1+\lambda)\cdot\left(R\dot{\theta}\right)^2 \tag{24}$$

The potential energy (both gravitational and elastic) of the system is

$$\begin{aligned} V = {} & 2Rg\cdot\left(m_b + m_t + N\frac{1}{2}m_c\right)\cos[\pm\alpha - \theta] + \frac{1}{2}m_t\omega_s^2\cdot(u_t - u_b)^2 + m_t\ddot{u}_g u_t \\ & -2R\ddot{u}_g\cdot\left(m_b + N\frac{1}{2}m_c\right)\sin[\pm\alpha - \theta] \end{aligned} \tag{25}$$

The virtual work performed by the damping force is

$$\delta W = f_D\cdot\delta q_i = -c\cdot(\dot{u}_t - \dot{u}_b)\cdot\delta u_t = -2\zeta_s m_t\omega_s\cdot(\dot{u}_t - \dot{u}_b)\cdot\delta u_t \tag{26}$$

Applying Eq. (18) to the degree of freedom of the superstructure, u_t, yields

$$\ddot{u}_t + 2\zeta_s\omega_s\cdot\left(\dot{u}_t - 2R\cdot\dot{\theta}\cos[\pm\alpha - \theta]\right) + \omega_s^2\cdot(u_t - 2R\cdot(\sin[\pm\alpha] - \sin[\pm\alpha - \theta])) = -\ddot{u}_g \tag{27}$$

A comparison of Eqs (11) and (27) shows that the displacement demand of the ground motion is now taken by both the rocking podium frame and the elastic superstructure. The equation of motion for the other degree of freedom, the rocking angle θ of the rocking frame that supports the superstructure, is

DOI: 10.1002/eqe

$$\begin{aligned}&\ddot{\theta}R\cdot\left(1+\lambda+4\gamma+4\gamma\eta\sin^2[\pm\alpha-\theta]\right)=\\&+2R\gamma\eta\dot{\theta}^2\sin(2[\pm\alpha-\theta])-g\cdot(2\gamma+2\gamma\eta+1)\sin[\pm\alpha-\theta]-\ddot{u}_g\cdot(2\gamma+1)\cos[\pm\alpha-\theta]\\&+2\gamma\eta\omega_s\cos[\pm\alpha-\theta]\cdot\left(\omega_s\cdot(u_t-2R\cdot(\sin[\pm\alpha]-\sin[\pm\alpha-\theta]))+2\zeta_s\cdot\left(\dot{u}_t-2R\cdot\dot{\theta}\cos[\pm\alpha-\theta]\right)\right)\end{aligned}\tag{28}$$

The equations present a similarity with several other problems of rocking–elasticity interaction [24, 28, 30, 53, 54].

3.4. Impacts and energy dissipation

The proposed dynamic model of a rocking podium structure has two degrees of freedom. Thus, two equations are needed to determine the post-impact condition and, thereby, the energy dissipated at impact. The model proposed by Housner [17] presumes that rocking column impacts are instantaneous and that the contact forces between the rocking column and the rocking surfaces are concentrated at the pivot points. Therefore, at the moment of impact, the pivot point instantaneously moves to the other edge of the column. This assumption has been previously used to calculate the coefficient of restitution in several rocking systems [46, 50, 55]. The aforementioned assumption results in Conservation of Angular Momentum (CoAM) for each column of the rocking podium frame during impact. Moreover, it is assumed that the elastic deformation of the superstructure is small compared with its size (height h_c), so CoAM is applied in the undeformed configuration of the rocking podium structure (Figure 5, left). This yields the first equation. The second equation comes from the assumption that the relative horizontal velocity between the superstructure mass and the cap beam does not change during impact.

Using the aforementioned assumptions, one can derive Eq. (29) for the coefficient of restitution and Eq. (30) for the horizontal velocity of the superstructure mass after impact:

$$c=\frac{\dot{\theta}^2_{\text{after}}}{\dot{\theta}^2_{\text{before}}}=\left[1-2\sin^2\alpha\cdot\frac{1+4\gamma\cdot(1+\eta)}{1+\lambda+4\gamma\cdot(1+\eta)}\right]^2\tag{29}$$

$$\dot{u}_{t,\text{after}}=\dot{u}_{t,\text{before}}-2R\cos\alpha\cdot\dot{\theta}_{\text{before}}\cdot\left(1-\sqrt{c}\right)\tag{30}$$

Equation (29) can be compared with the expressions for the coefficient of restitution of other, simpler, rocking systems. With $\eta = \gamma = 0$, for example, it yields exactly what Housner proposed for his rigid block, and with $\eta = 0$, its solution is equal to the expression of Makris and Vassiliou [46] for a rocking frame.

Different impact assumptions have also been proposed for deformable rocking structures [24, 27, 28, 53], but their thorough investigation is beyond the scope of this study.

3.5. Frequency in the uplifted state

As has been shown both analytically [28, 30, 31, 56] and experimentally [25, 32, 34, 57], the natural frequency of an uplifted structure $\omega_{s,u}$ is larger than the fixed-base frequency ω_s of the same structure. This supports the assumption of a 'rigid-body superstructure' found in [3]. The uplifted frequency can be computed through eigenfrequency analysis of the rocking podium structure:

$$\left|\mathbf{K}-\omega^2_{s,u}\mathbf{M}\right|=0\tag{31}$$

where $\mathbf{K}$ is the stiffness matrix and $\mathbf{M}$ is the mass matrix of the rocking podium structure. In the presence of damping, the aforementioned equation needs to be correct only if damping satisfies the Caughey–O'Kelly condition [32], which is not the case. However, since the superstructure remains elastic, the energy dissipated through its motion (its damping) is expected to be relatively small compared with the energy dissipated by the rocking of the podium frame, and, therefore, Eq. (31) is expected to give a good approximation of the uplifted frequencies. This was experimentally confirmed for other elastic uplifting systems [32, 34, 57].

DOI: 10.1002/eqe

Linearizing the equations of motion of the rocking podium structure (Eqs. (27) and (28)) and neglecting gravity yield the mass and stiffness matrices of the system:

$$\mathrm{M} = \begin{bmatrix} R\cdot\left[1+\lambda+4\gamma+4\gamma\eta\sin^2\alpha\right] & 0 \\ 0 & 1 \end{bmatrix}, \quad \mathrm{K} = \begin{bmatrix} 4R\gamma\eta\omega_s^2\cos^2\alpha & -2\gamma\eta\omega_s^2\cos\alpha \\ -2R\omega_s^2\cos\alpha & \omega_s^2 \end{bmatrix} \tag{32}$$

Solving the eigenvalue problem (Eq. (31)) gives

$$\omega_{s,u}^4\cdot\left(1+\lambda+4\gamma+4\gamma\eta\sin^2\alpha\right) - \omega_{s,u}^2\omega_s^2\cdot(1+\lambda+4\gamma+4\gamma\eta) = 0 \tag{33}$$

The eigenfrequency analysis reveals the two distinct mode shapes of the uplifted rocking podium structure. The first one is a rotation of the podium frame columns with a natural frequency of 0 Hz, a rigid body mode. The second one is the vibration of the elastic SDOF system when the rocking podium frame is uplifted (Figure 5, right). In this uplifted state, the natural eigenfrequency $\omega_{s,u}$ of the SDOF system is

$$\omega_{s,u} = \sqrt{\frac{1+\lambda+4\gamma\cdot(1+\eta)}{1+\lambda+4\gamma\cdot\left(1+\eta\sin^2\alpha\right)}}\cdot\omega_s \tag{34}$$

Clearly, the natural frequency of the uplifted SDOF system $\omega_{s,u}$ is larger than its fixed-base frequency ω_s. For heavy superstructures ($\eta\to\infty$) (i.e., large number of stories), the amplification factor simplifies to $1/\sin(\alpha)$, which coincides with the solution of Yim and Chopra [56] for structures with foundation uplift.

Figure 7 (left) plots the superstructure vibration frequency amplification factor for different values against the superstructure mass ratio for the three superstructure mass ratio values, effectively representing the number of stories above the rocking podium frame. It can be seen that the eigenfrequencies of superstructures with more stories experience larger amplification when the podium is uplifted. However, assuming that the fixed-base natural frequency of a building is given by the empirical relation f_n = 10 Hz/n_s (where n_s is the number of stories), one can prove that the uplifted frequency of the superstructure decreases with increasing number of stories. Since a planar model is used to represent the in-plane behavior of a 3D podium structure, the cap beam represents the mass of a whole slab. Typically, this slab is much heavier than the total weight of the columns, so γ is expected to have a large value. Therefore, it is reasonable to assume that the eigenfrequencies of the superstructure when the podium is in the uplifted state are given by the limit of Eq. (34) as $\gamma\to\infty$:

$$\omega_{s,u} = \sqrt{\frac{1+\eta}{1+\eta\sin^2\alpha}}\cdot\omega_s \tag{35}$$

Figure 7 (right) plots Eq. (35) for different values of column slenderness α, assuming γ = 10.

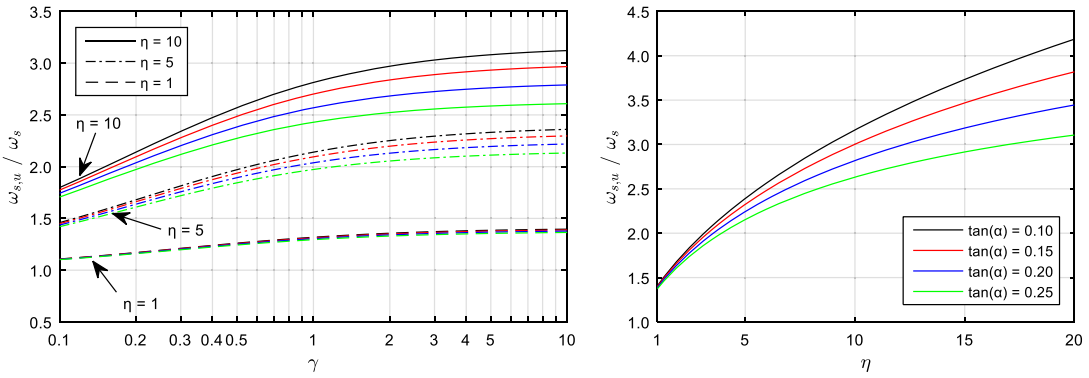

Figure 7. Amplification factor for the natural frequency ω_s of the elastic superstructure on a rocking podium frame in the uplifted (rocking) state: variation with respect to the beam mass ratio γ (left) and variation with respect to the superstructure mass ratio η, given γ = 10 (right).

DOI: 10.1002/eqe

3.6. Damping in the uplifted state

As in [28, 30, 32, 56], the assumption of viscous damping of the superstructure leads to a damping ratio in the uplifted state equal to

$$\zeta_{s,u} = \sqrt{\frac{1+\lambda+4\gamma\cdot(1+\eta)}{1+\lambda+4\gamma\cdot\left(1+\eta\sin^2\alpha\right)}}\cdot\zeta_s = S_r\cdot\zeta_s \tag{36}$$

However, the results of experiments [34] show that uplifting of a deformable rocking column may not affect its damping. Therefore, it is reasonable to assume that the forces representing energy dissipation in the equation of motion of the superstructure are not proportional to the elastic velocity of the superstructure. However, since damping in the superstructure is expected to be small, [34] suggests to use viscous damping equal to ζ_s/S_r so that damping in the uplifted (amplified) state is equal to ζ_s.

4. DIMENSIONAL ANALYSIS OF THE ROCKING PODIUM STRUCTURE MODEL

Strong ground motions often contain a distinguishable acceleration pulse, which is responsible for most of the inelastic deformation of fixed-base structures [58–60]. Physically realizable ground motion analytical pulses can qualitatively describe the impulsive character of near-fault ground motions. For a particular pulse shape, two parameters are needed to describe such pulses. The acceleration amplitude, a_p, and dominant cyclic frequency, ω_p, of the pulse, or the velocity amplitude, v_p, and dominant cyclic frequency, ω_p, have been previously used [59]. This section examines the response of the rocking podium structure model shown in Figure 5 to an idealized acceleration pulse characterized by its amplitude, a_p, and dominant cyclic frequency, ω_p [61]. The tilt angle response is a function of 10 variables:

$$\theta = f\left(\alpha, R, g, \omega_p, a_p, \eta, \gamma, \omega_s, \zeta_s, t\right) \tag{37}$$

involving two fundamental dimensions. According to Buckingham's Π theorem [62], the response can be described by $10 - 3 = 7$ dimensionless parameters. Combining the Π theorem with orientational analysis arguments [63] and taking into account that $\tan(\alpha)$ is bijective for $0 < \alpha < \pi/2$, the problem can be described as

$$\frac{\theta}{\alpha} = \varphi\left(\alpha, \frac{\omega_p}{p}, \frac{a_p}{g\tan\alpha}, \eta, \gamma, \frac{\omega_s}{p}, \zeta_s, \tau\right) \tag{38}$$

where $\tau = pt$ and p is defined by Eq. (2).

4.1. Range of interest of the dimensionless parameters

- *Column slenderness tan(α)*: Since $\tan(\alpha)$ controls the superstructure design forces, in order for the rocking podium structure to work as a useful seismic isolation system, α cannot be excessively large. Typically, slenderness values $\tan(\alpha) < 0.3$ are meaningful.
- *Size-frequency parameter ω_p/p*: Ideal candidates for rocking isolation, such as tall bridges and chimneys, can have a height reaching several tens of meters. However, in the model under study, typical rocking podium columns are expected to have a height of no more than 6 m. A value of $\omega_p/p = 8$ corresponds to a pulse period of 0.5 s for a 6-m-tall column. Therefore, values of $\omega_p/p < 8$ will be examined.
- *Dimensionless masses η and γ*: For superstructure floors of equal mass, η corresponds to the number of floors. Superstructures with up to 10 floors (for rocking spectra) and up to five floors (for time history analysis) are analyzed. As previously explained, γ is expected to be large as it represents a slab-to-columns mass ratio. Figure 7 (left) shows that the frequency amplification ratio has already saturated for $\gamma = 10$, so γ is set to equal to 10.

DOI: 10.1002/eqe

- *Dimensionless superstructure stiffness* ω_s/p: A lower bound for ω_s/p is derived by minimizing ω_s and maximizing p (i.e., minimizing rocking column height). Therefore, a lower bound of ω_s/p is obtained by assuming a 10-story superstructure placed on a 3-m-tall rocking podium. Then, the fundamental period of the superstructure is on the order of 1 s and $\omega_s/p \approx 3$. For the results presented in this paper, a lower bound of $\omega_s/p = 3$ is chosen.
- *Superstructure damping ratio*: The superstructure is intended to remain elastic during its response to design-basis excitation. Therefore, its fixed-base structural damping is expected to be no larger than 0.01. According to Section 3.6, $\zeta_s = 0.01/S_r$ is used. This way, the uplifted damping will be constant and equal to 0.01.

5. RESPONSE OF THE ROCKING PODIUM STRUCTURE TO ANALYTICAL PULSE GROUND MOTIONS

The second derivative of the Gaussian distribution, $\exp(-t^2/2)$, known in the seismological literature as the symmetric Ricker wavelet [64],

$$\ddot{u}_g(t) = a_p\left(1 - \frac{2\pi^2 t^2}{T_p^2}\right)e^{-\frac{1}{2}\frac{2\pi^2 t^2}{T_p^2}} \tag{39}$$

plotted in Figure 8 (right), has often been used to approximate the pulses contained in pulse-like ground motions. The value of the pulse period $T_p = 2\pi/\omega_p$ maximizes the Fourier spectrum of the symmetric Ricker wavelet. Similarly, Eq. (40) is the scaled third derivative of the Gaussian distribution $\exp(-t^2/2)$, also referred to as the antisymmetric Ricker wavelet (Figure 8, left), in which factor β is equal to 1.3801 to enforce that the function maximum is equal to a_p.

$$\ddot{u}_g(t) = \frac{a_p}{\beta}\left(\frac{4\pi^2 t^2}{3T_p^2} - 3\right)\frac{2\pi t}{\sqrt{3}T_p}e^{-\frac{1}{2}\frac{4\pi^2 t^2}{3T_p^2}} \tag{40}$$

Figures 9 and 10 show the maximum rocking angle response spectra for antisymmetric and symmetric Ricker wavelet excitations. From left to right, the weight of the superstructure (i.e., the number of stories), defined by Eq. (10), is increased ($\eta \in \{1, 5, 10\}$). From top to bottom, the natural period T_s of the superstructure SDOF model is increased from 0 s (rigid) to 0.95 s (deformable) ($\omega_s/p \in \{\infty, 30, 6, 3\}$). The podium cap beam-to-column mass ratio is chosen as $\gamma = 10$ as it was found that its further increase does not influence the response (Figure 7, left). The column slenderness used to compute the rocking spectra is $\tan(\alpha) = 0.15$. Results of analyses for other slenderness values, not presented here because of space limits, show that the rocking podium spectra are not sensitive to this parameter. The mass eccentricity factor λ is set to 1/3 (uniformly distributed column mass). Although a new size parameter $\tilde{p}$, that also takes γ into account, was introduced with Eq. (8), the lower x-axes of the spectra show the value of the pulse natural frequency ω_p normalized by p, which corresponds to the frequency parameter of a column with evenly distributed mass and semi-diagonal R, defined by Eq. (2). To give a sense of the magnitude of the non-dimensional term ω_p/p, the pulse period, T_p, that corresponds to $p = 2.2\ \mathrm{s}^{-1}$ (column with $2H = 3$ m) is plotted on the top horizontal axis. In order to test the second design guideline of Polyakov [3], that is, the rocking frame should be treated as a very flexible elastic structure; the spectra in Figures 9 and 10 also plot

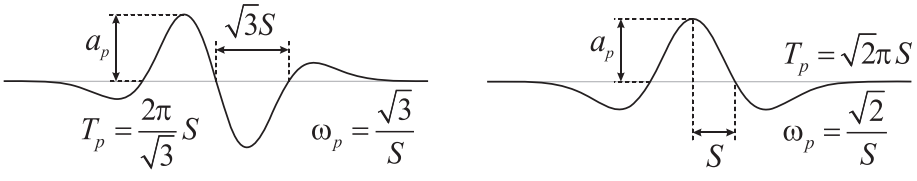

Figure 8. Analytical pulses: antisymmetric Ricker wavelet (left) and symmetric Ricker wavelet (right).

DOI: 10.1002/eqe

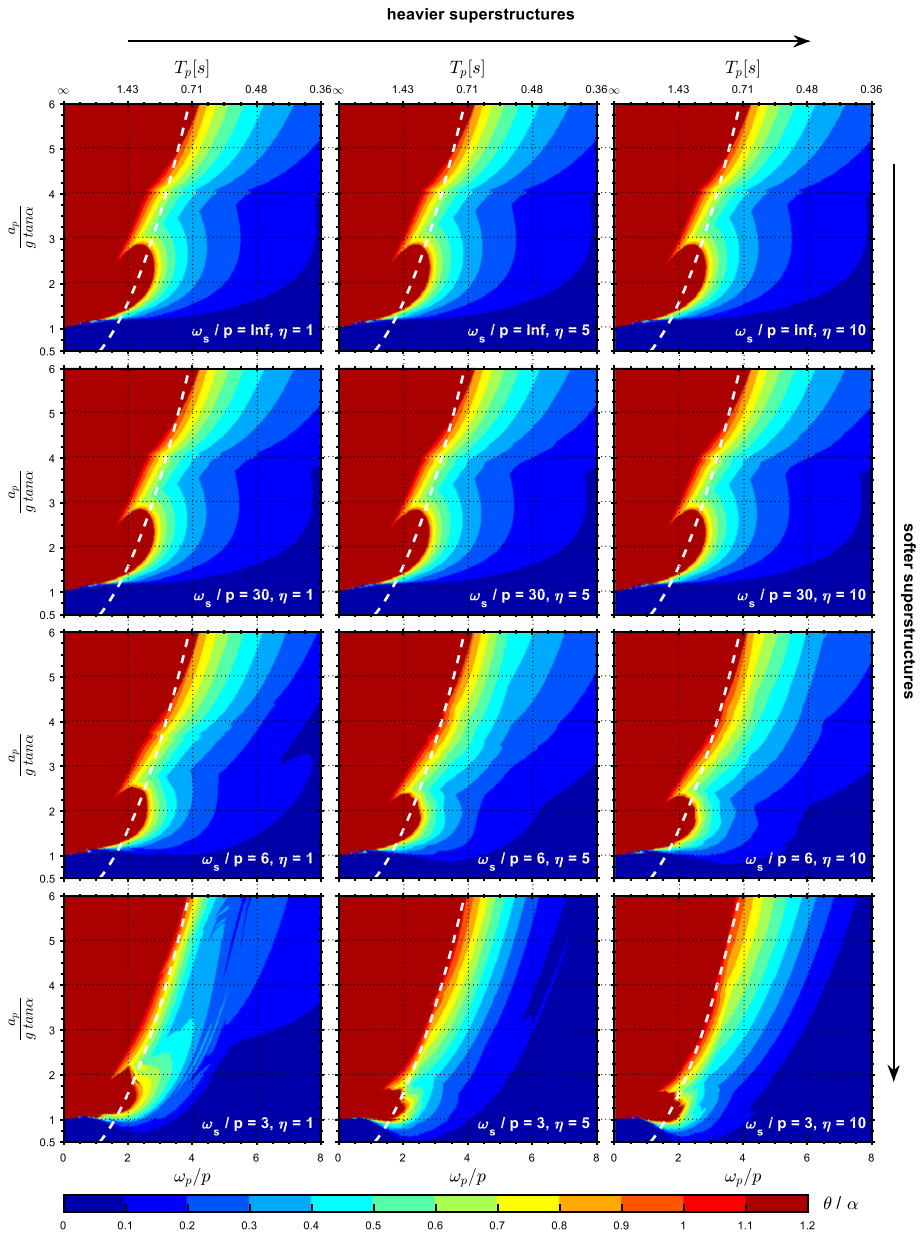

Figure 9. Rocking spectra (maximum base rotation, θ/α) of a rocking podium structure with γ = 10 and different values of ω_s/p (∞, 30, 6, 3) and η (1, 5, 10) subjected to an antisymmetric Ricker wavelet. The white dashed line indicates Polyakov's overturning acceleration.

(white dashed lines) the pulse acceleration that would cause a displacement of the system (measured at the top of the rocking columns) equal to the column total width ($2B$) and would, therefore, cause collapse. This design guideline is consistent to what [65–67] propose.

Figure 11 plots the minimum overturning acceleration spectra for both symmetric and antisymmetric Ricker wavelet excitation. It shows that the interaction between the rocking podium frame and the elastic superstructure follows similar trends as the ones observed in [28, 30].

1. For low values of ω_p/p (small height of the rocking podium frame or low-frequency pulses), the deformability of the superstructure has a detrimental effect on the stability of the system, while the opposite holds for high values of ω_p/p.

DOI: 10.1002/eqe

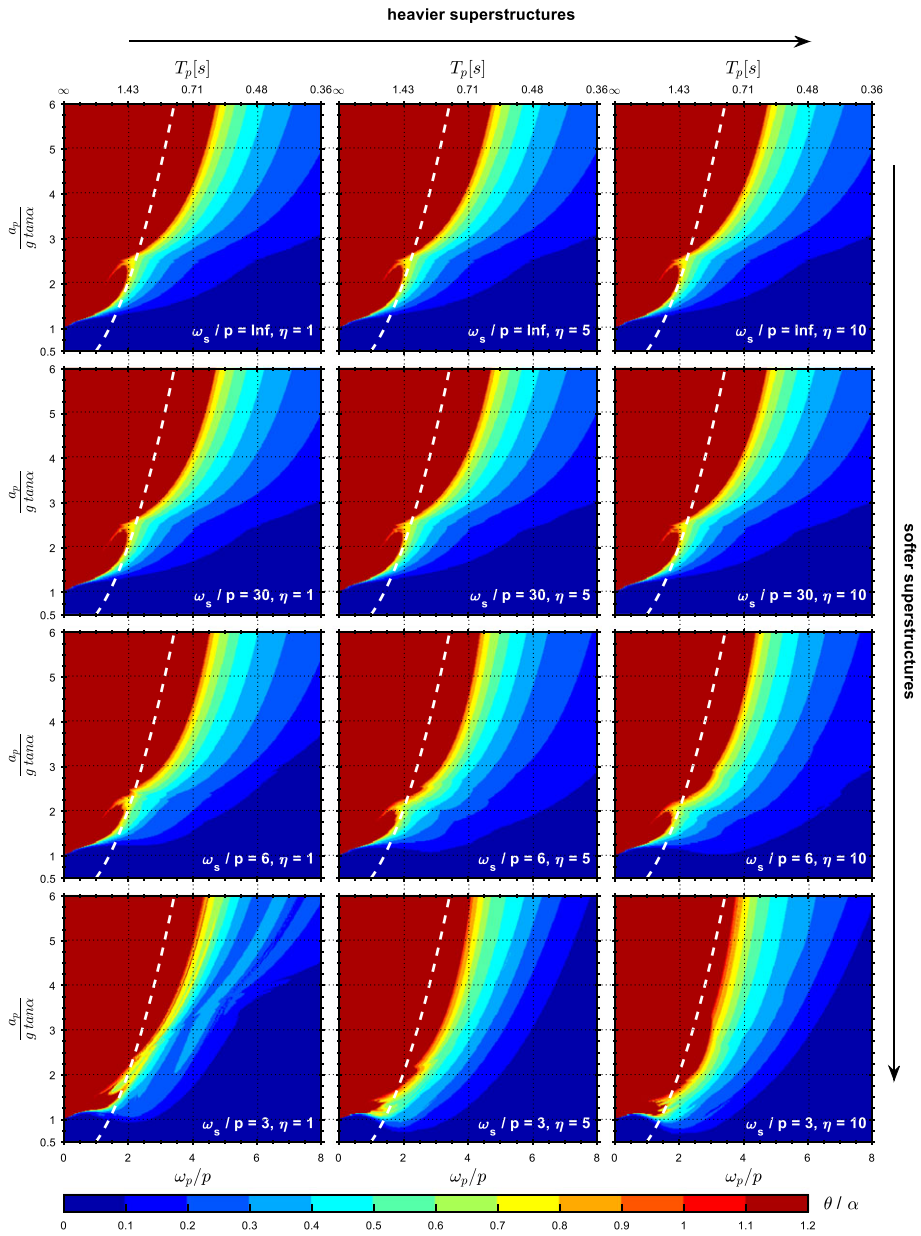

Figure 10. Rocking spectra (maximum base rotation, θ/α) of a rocking podium structure with γ = 10 and different values of ω_s/p (∞, 30, 6, 3) and η (1, 5, 10) subjected to a symmetric Ricker wavelet. The white dashed line indicates Polyakov's overturning acceleration.

2. For low values of ω_p/p, the deformability of the superstructure clearly decreases the acceleration needed to cause uplift.
3. The effects of the superstructure deformability become negligible for $\omega_s/p > 6$. For 3-m-tall columns, this value of ω_s/p corresponds to a structural period, T_s, equal to 0.48 s.
4. The weight of the superstructure has only a marginal influence on the system stability.

Based on these findings, the first Polyakov [3] guideline (to treat the superstructure of rocking podium structures as a rigid body) is reasonable, at least for superstructures with natural periods shorter than 0.48 s (for a rocking column height equal to 3 m).

For values of $\omega_p/p < 1.8$, the second Polyakov guideline (modeling the rocking story as a very flexible elastic oscillator) is conservative. However, for larger values of ω_p/p (corresponding to pulse

DOI: 10.1002/eqe

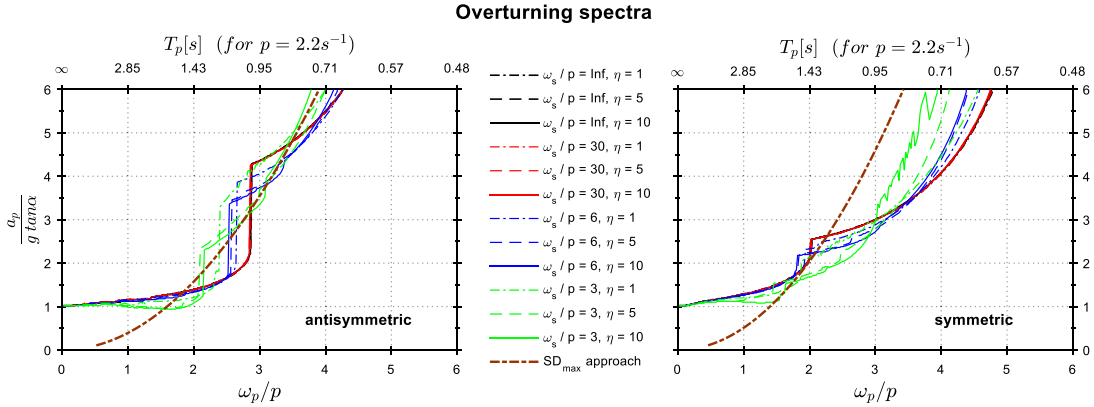

Figure 11. Overturning spectra for a rocking podium structure subjected to Ricker wavelets: antisymmetric Ricker (left) and symmetric Ricker (right).

periods smaller than about 1.6 s for 3-m-tall columns of the rocking frame), analytical pulse analysis suggests that this assumption become non-conservative and should clearly be avoided.

6. RESPONSE OF THE ROCKING PODIUM STRUCTURE TO RECORDED GROUND MOTIONS

Recorded ground motions might or might not contain acceleration pulses. Even in the case of pulse-like ground motions, the pulse itself cannot entirely describe the overturning potential of the ground motion [38]. Therefore, the analysis presented in the previous section provides only qualitative conclusions. In order to further explore the stability of rocking podium structures and to further check the validity of the design rules of thumb proposed by Polyakov [3], the model presented in this paper is excited with recorded ground motions.

A model with a 3-m-tall rocking frame that supports either a one-story (η = 1, T_s = 0.1 s) or five-story (η = 5, T_s = 0.5 s) superstructure. In order to have different displacement capacities of the rocking columns, models with column slenderness of 0.15 (used for Ricker pulse analyses) as well as 0.10 and 0.20 are analyzed. According to Polyakov's design guidelines [3], a rocking column is stable as long as the maximum of ground motion elastic displacement spectrum, $SD_{\max}$, is smaller than the width of the column $2B$ (e.g., $2B$ = 0.60 m for $\tan(\alpha)$ = 0.20). A viscous damping ratio of 2% was used to compute the ground motion elastic displacement spectra. This should not be confused with the superstructure damping. It is the viscous damping of Polyakov's equivalent linear system that is intended to approximate the damping of the rocking story.

Tables I and II show the recorded ground motions from the Next Generation Attenuation (NGA) [68] database that were used to investigate the response of rocking podium structures for pulse-like (group A) and non-pulse-like (group B) ground motions. The records are chosen such that $SD_{\max}$ values, shown in the last column of the tables, vary sufficiently to cover different displacement capacities ($2B$ either 0.30, 0.45, or 0.60 m) of the podium structure columns.

In general, the maximum spectral displacement approach proposed by Polyakov [3] leads to a conservative design. Figure 12 compares the maximum displacement at the top of the rocking podium columns $u_{b\max}$ computed in the ground motion response history analyses using the proposed rocking podium structure model to the maximum elastic spectral displacement for each of the 126 conducted analyses, both normalized by $2B$. According to [3], $SD_{\max} > 2B$ corresponds to overturning. Points above the $u_{b\max}/2B = 1$ line correspond to overturning according to the rocking podium model, while points right of the $SD_{\max}/2B = 1$ line correspond to overturning according to the maximum elastic spectral displacement. For points below the diagonal, the $SD_{\max}$ approach is conservative, while the opposite holds for points above the diagonal. There are many ground motions for which the $SD_{\max}$ approach predicts overturning while the rocking podium structure

DOI: 10.1002/eqe

Table I. Pulse-like ground motions used for the rocking podium structure seismic response analysis.

No.	Earthquake	Year	Station	NGA file name	PGA (g)	$SD_{\max}$ (m)
A1	Parkfield	1966	C #2/065	00029L	0.48	0.46
A2	San Fernando	1971	Pacoima Dam/164	00077L	1.23	1.06
A3	San Salvador	1986	Geotech Invest Center/180	00568T	0.48	0.36
A4	Whittier Narrows	1987	LB-Orange Ave/010	00645L	0.26	0.14
A5	Spitak	1988	Gukasian/000	00730L	0.20	0.31
A6	Loma Prieta	1989	Oakland, outer Harbor Wharf/000	00783L	0.29	0.33
A7	Erzincan	1992	Erzincan/NS	00821L	0.52	0.94
A8	Erzincan	1992	Erzincan/EW	00821T	0.50	0.85
A9	Landers	1992	Yermo Fire Station/270	00900L	0.24	1.19
A10	Landers	1992	Yermo Fire Station/360	00900T	0.15	0.70
A11	Northridge	1994	Jensen Filter Plant Gen BLDG/022	00983L	0.56	1.25
A12	Kobe	1995	Takarazuka/000	01119L	0.69	0.77
A13	Kobe	1995	Takarazuka/090	01119T	0.69	0.55

Table II. Non-pulse-like ground motions used for the rocking podium structure seismic response analysis.

No.	Earthquake	Year	Station	NGA file name	PGA (g)	$SD_{\max}$ (m)
B1	Imperial Valley	1940	Imperial Valley/180	00006L	0.31	0.37
B2	Imperial Valley	1940	Imperial Valley/270	00006T	0.21	0.64
B3	San Fernando	1971	Pacoima Dam/254	00077T	1.16	0.36
B4	San Salvador	1986	Geotech Invest Center/090	00568L	0.87	0.46
B5	Whittier Narrows	1987	LB-Orange Ave/280	00645T	0.15	0.07
B6	Spitak	1988	Gukasian/090	00730T	0.18	0.18
B7	Loma Prieta	1989	Oakland, outer Harbor Wharf/270	00783T	0.27	0.46
B8	Northridge	1994	Jensen Filter Plant Gen BLDG/292	00983T	1.04	0.70

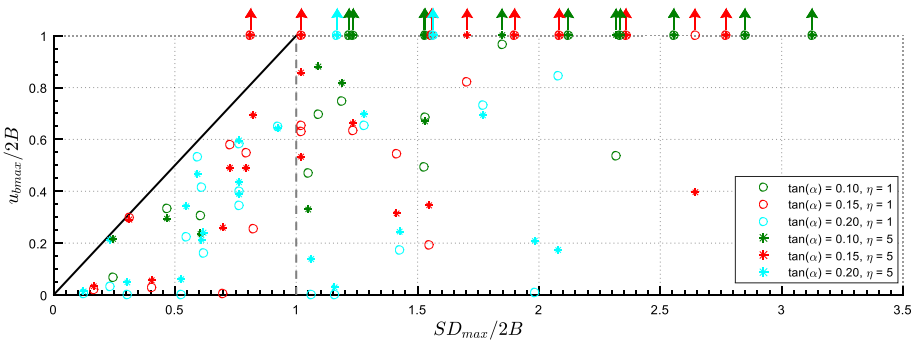

Figure 12. Results of earthquake ground motion response history analyses: maximum top column displacement $u_{b\max}$ versus maximum elastic spectral displacement $SD_{\max}$.

model does not. However, out of 126 response history analyses, there were only two false-negative (i.e., unconservative) overturning predictions. The transverse-direction record of the 1986 San Salvador earthquake (no. A3) overturns both rocking podium buildings ($\eta = 1$ and $\eta = 5$) with columns with a slenderness of $\tan(\alpha) = 0.15$ in a response history analysis. However, Polyakov's $SD_{\max}/2B = 0.36$ m/0.45 m $= 0.80 < 1$ criterion indicates the buildings should survive this earthquake ground motion.

DOI: 10.1002/eqe

In contrast to the responses to analytical pulse ground motions, the responses of the rocking podium structures to recorded ground motions are more sensitive to the column slenderness parameter. It seems that the high-frequency incoherent component of the ground motion is oftentimes able to induce column uplift and initiate the rocking motion earlier. This observation parallels the conclusion for elastic rocking structures with similar column sizes [27].

The ground motion analysis results also reveal that the $SD_{\max}$ approach gives conservative results in a larger range of pulse frequencies than the analytical pulse analysis shows. Namely, analytical pulse analysis predicts that the $SD_{\max}$ approach is unconservative for $\omega_p/p > 1.8$ (i.e., for 3-m-tall rocking podium frame columns, the approach is unconservative for pulses with pulse period $T_p < 1.6$ s) (Figure 11). However, the Erzincan (A7) and the Northridge (A11) pulses have frequencies on the order of 0.9 and 0.5 s, respectively, and still, the maximum elastic spectral displacement approach is conservative. It seems that, for the ground motions used, the incoherent high-frequency component of the ground motion increased $SD_{\max}$ more than it increased the overturning potential of the ground motion.

7. CONCLUSIONS

Rocking podium structures comprise a superstructure anchored on top of a rigid slab supported by free-standing columns that can uplift and undergo rocking motion in response to sufficiently strong ground motion excitation. A dynamic model that describes the in-plane seismic response of such structures (Figure 5) was derived and presented in this paper. This model was used to analyze the seismic response of a wide range of rocking podium structures to analytical pulse and recorded ground motion excitations. The computed responses indicate that rocking podium structures remain stable under ground motion excitation and that the rule-of-thumb guidelines of Polyakov [3] are conservative in most of the cases examined.

The equivalent seismic forces acting on the superstructure are controlled by the dimensions of the rocking podium columns. Determining the magnitude of these forces requires more accurate models of the rocking podium and the superstructure and is the focus of ongoing research.

REFERENCES

1. Beck JL, Skinner RI. The seismic response of a reinforced concrete bridge pier designed to step. *Earthquake Engineering and Structural Dynamics* 1973, **2**(4):343–358. https://doi.org/10.1002/eqe.4290020405.
2. Sharpe RD, Skinner RI. The seismic design of an industrial chimney with rocking base. *Bulletin of the New Zealand National Society for Earthquake Engineering* 1983, **16**(2):98–106.
3. Polyakov SV. *Design of Earthquake Resistant Structures*. English tr. Moscow: MIR Publishers; 1974.
4. Huckelbridge A, Clough R. *Earthquake Simulation Tests of a Nine Story Steel Frame with Columns Allowed to Uplift*. 1977.
5. Ricles JM, Sause R, Garlock MM, Zhao C. Posttensioned seismic-resistant connections for steel frames. *Journal of Structural Engineering* 2001, **127**(2):113–121 https://doi.org/10.1061/(ASCE)0733-9445(2001)127:2(113).
6. Priestley M, Sritharan S, Conley J, Pampanin S. Preliminary Results and Conclusions from the PRESSS Five-story Precast Concrete Test Building. 1999.
7. Liu R, Palermo A. Low damage design and seismic isolation: what's the difference? 2015 NZSEE Conference, 2015.
8. Vassiliou MF, Makris N. Dynamics of the vertically restrained rocking column. *Journal of Engineering Mechanics* 2015, **141**(12): 4015049. https://doi.org/10.1061/(ASCE)EM.1943-7889.0000953.
9. Makris N, Vassiliou MF. Dynamics of the rocking frame with vertical restrainers. *Journal of Structural Engineering* 2015, **141**(10): 4014245. https://doi.org/10.1061/(ASCE)ST.1943-541X.0001231.
10. Giouvanidis AI, Dimitrakopoulos EG. Seismic performance of rocking frames with flag-shaped hysteretic behavior. *Journal of Engineering Mechanics* 2016; accepted 5 OCT.
11. Zeris C. Seismic response of rocking oscillators on a soft story: elastic response. *Journal of Structural Engineering* 2015, **141**(8): 4014196. https://doi.org/10.1061/(ASCE)ST.1943-541X.0001157.
12. Cherepinskiy Y. Seismic isolation of buildings with application of the kinematics bases. 13th World Conference on Earthquake Engineering, 2004.
13. Uzdin AM, Doronin FA, Davydova GV, Avidon GE, Karlina EA. Performance analysis of seismic-insulating elements with negative stiffness. *Soil Mechanics and Foundation Engineering* 2009, **46**(3):15–21.
14. Semenov S, Kurzanov A. Kinematic base isolation systems 2011. https://www.youtube.com/watch?v=Tqr0k4Dw2FM [accessed March 1, 2016].
15. Semenov S. Сейсмоизоляция protection against earthquake 2015. https://www.youtube.com/watch?v=sZ5KCX2wMd0 [accessed March 1, 2016].

DOI: 10.1002/eqe

16. Priestley M, Evison R, Carr A. Seismic response of structures free to rock on their foundations. *Bulletin of the New Zealand National* 1978, 141–150.
17. Housner GW. The behavior of inverted pendulum structures during earthquakes. *Bulletin of the Seismological Society of America* 1963, **53**(2):403–417.
18. Dimitrakopoulos EG, DeJong MJ. Overturning of retrofitted rocking structures under pulse-type excitations. *Journal of Engineering Mechanics* 2012, **138**(8):963–972. https://doi.org/10.1061/(ASCE)EM.1943-7889.0000410.
19. Yim CS, Chopra AK, Penzien J. Rocking response of rigid blocks to earthquakes. *Earthquake Engineering and Structural Dynamics* 1980, **8**(6):565–587. https://doi.org/10.1002/eqe.4290080606.
20. Psycharis IN, Jennings PC. Rocking of slender rigid bodies allowed to uplift. *Earthquake Engineering and Structural Dynamics* 1983, **11**(1):57–76. https://doi.org/10.1002/eqe.4290110106.
21. Zhang J, Makris N. Rocking response of free-standing blocks under cycloidal pulses. *Journal of Engineering Mechanics* 2001, **127**(5):473–483. https://doi.org/10.1061/(ASCE)0733-9399(2001)127:5(473).
22. Makris N, Vassiliou MF. Sizing the slenderness of free-standing rocking columns to withstand earthquake shaking. *Archive of Applied Mechanics* 2012, **82**(10–11):1497–1511. https://doi.org/10.1007/s00419-012-0681-x.
23. Dimitrakopoulos EG, Fung EDW. Closed-form rocking overturning conditions for a family of pulse ground motions. Proceedings of the Royal Society A, 2016.
24. Oliveto G, Caliò I, Greco A. Large displacement behaviour of a structural model with foundation uplift under impulsive and earthquake excitations. *Earthquake Engineering and Structural Dynamics* 2003, **32**(3):369–393. https://doi.org/10.1002/eqe.229.
25. Ma QTM. *The Mechanics of Rocking Structures Subjected to Ground Motion*. 2010.
26. Vassiliou MF, Mackie KR, Stojadinović B. Dynamic response analysis of solitary flexible rocking bodies: modeling and behavior under pulse-like ground excitation. *Earthquake Engineering and Structural Dynamics* 2014, **43**(10):1463–1481. https://doi.org/10.1002/eqe.2406.
27. Acikgoz S, DeJong MJ. The rocking response of large flexible structures to earthquakes. *Bulletin of Earthquake Engineering* 2014, **12**(2):875–908. https://doi.org/10.1007/s10518-013-9538-0.
28. Vassiliou MF, Truniger RE, Stojadinović B. An analytical model of a deformable cantilever structure rocking on a rigid surface: development and verification. *Earthquake Engineering and Structural Dynamics* 2015, **44**(13). https://doi.org/10.1002/eqe.2608.
29. Wiebe L, Christopoulos C. A cantilever beam analogy for quantifying higher mode effects in multistorey buildings. *Earthquake Engineering and Structural Dynamics* 2015, **44**(11):1697–1716.
30. Acikgoz S, DeJong MJ. The interaction of elasticity and rocking in flexible structures allowed to uplift. *Earthquake Engineering and Structural Dynamics* 2012, **41**(11):1–18. https://doi.org/10.1002/eqe.2181.
31. Acikgoz S, Dejong M. An investigation of the dynamics of rocking isolation for earthquake-resilient design. ECCOMAS Congress 2016: 7th European Congress on Computational Methods in Applied Sciences and Engineering, 2016.
32. Acikgoz S, DeJong MJ. Analytical modelling of multi-mass flexible rocking structures. *Earthquake Engineering and Structural Dynamics* 2016, **41**(11):1549–1568 https://doi.org/10.1002/eqe.2735.
33. Peña F, Prieto F, Lourenço PB, Campos Costa A, Lemos JV. On the dynamics of rocking motion of single rigid-block structures. *Earthquake Engineering and Structural Dynamics* 2007, **36**(15):2383–2399. https://doi.org/10.1002/eqe.739.
34. Truniger RE, Vassiliou MF, Stojadinović B. An analytical model of a deformable cantilever structure rocking on a rigid surface: experimental validation. *Earthquake Engineering and Structural Dynamics* 2015, **44**(13). https://doi.org/10.1002/eqe.2609.
35. Bachmann JA, Bloechlinger P, Wellauer M, Vassiliou MF, Stojadinovic B. Experimental investigation of the seismic response of a column rocking and rolling on a concave base. ECCOMAS Congress 2016: 7th European Congress on Computational Methods in Applied Sciences and Engineering, Heraklion: 2016.
36. Giouvanidis AI, Dimitrakopoulos EG. Nonsmooth dynamic analysis of sticking impacts in rocking structures. *Bulletin of Earthquake Engineering* 2017, **15**(5):2273–2304. https://doi.org/10.1007/s10518-016-0068-4.
37. Psycharis IN, Fragiadakis M, Stefanou I. Seismic reliability assessment of classical columns subjected to near-fault ground motions. *Earthquake Engineering and Structural Dynamics* 2013, **42**(14):n/a–n/a https://doi.org/10.1002/eqe.2312.
38. Dimitrakopoulos EG, Paraskeva TS. Dimensionless fragility curves for rocking response to near-fault excitations. *Earthquake Engineering and Structural Dynamics* 2015, **44**(12):2015–2033. https://doi.org/10.1002/eqe.2571.
39. Bakhtiary E, Gardoni P. Probabilistic seismic demand model and fragility estimates for rocking symmetric blocks. *Engineering Structures* 2016, **114**:25–34. https://doi.org/10.1016/j.engstruct.2016.01.050.
40. Mander JB, Cheng CT. Seismic resistance of bridge piers based on damage avoidance design. 1997.
41. Sakai J, Mahin SA. *Analytical Investigations of New Methods for Reducing Residual Displacements of Reinforced Concrete Bridge Columns*. Pacific Earthquake Engineering Research Center: Berkeley, CA, 2004.
42. Wacker JM, Hieber DG, Stanton JF, Eberhard MO. Design of precast concrete piers for rapid bridge construction in seismic regions. *Research in Reproduction* 2005.
43. Cheng CT. Shaking table tests of a self-centering designed bridge substructure. *Engineering Structures* 2008, **30**(12):3426–3433.
44. Kokkali P, Abdoun T, Anastasopoulos I. Centrifuge modeling of rocking foundations on improved soil. *Journal of Geotechnical and Geoenvironmental Engineering* 2015, **141**(10): 4015041.

DOI: 10.1002/eqe

45. Makris N, Konstantinidis D. The rocking spectrum and the limitations of practical design methodologies. *Earthquake Engineering and Structural Dynamics* 2003, **32**(2):265–289. https://doi.org/10.1002/eqe.223.
46. Makris N, Vassiliou MF. Planar rocking response and stability analysis of an array of free-standing columns capped with a freely supported rigid beam. *Earthquake Engineering and Structural Dynamics* 2013, **42**(3):431–449. https://doi.org/10.1002/eqe.2222.
47. Makris N, Vassiliou MF. Are some top-heavy structures more stable? *Journal of Structural Engineering* 2014, **140**(5): 6014001. https://doi.org/10.1061/(ASCE)ST.1943-541X.0000933.
48. Papaloizou L, Komodromos P. Planar investigation of the seismic response of ancient columns and colonnades with epistyles using a custom-made software. *Soil Dynamics and Earthquake Engineering* 2009, **29**(11–12):1437–1454. https://doi.org/10.1016/j.soildyn.2009.06.001.
49. Vassiliou MF, Mackie KR, Stojadinović B. A finite element model for seismic response analysis of deformable rocking frames. *Earthquake Engineering and Structural Dynamics* 2016; https://doi.org/10.1002/eqe.2799.
50. Dimitrakopoulos EG, Giouvanidis AI. Seismic response analysis of the planar rocking frame. *Journal of Engineering Mechanics* 2015, **141**(7): 4015003. https://doi.org/10.1061/(ASCE)EM.1943-7889.0000939.
51. Eisenberg JM, Smirnov VI, Bubis AA. Recent developments in seismic isolation and energy dissipation in Russia. 14th World Conference on Earthquake Engineering, 2008.
52. Eisenberg JM, Smirnov VI. Building seismic isolation in Russia without rubber and with rubber. ISET Golden Jubilee Symposium, 2012.
53. Psycharis IN. Effect of base uplift on dynamic response of SDOF structures. *Journal of Structural Engineering* 1991, **117**(3):733–754. https://doi.org/10.1061/(ASCE)0733-9445(1991)117:3(733).
54. Simoneschi G, de Leo AM, Di Egidio A. Effectiveness of oscillating mass damper system in the protection of rigid blocks under impulsive excitation. *Engineering Structures* 2017, **137**:285–295.
55. Makris N, Vassiliou MF. Rocking response and stability analysis of an array of free-standing columns capped with a free-standing rigid beam. *COMPDYN* 2013, **2013**.
56. Chopra AK, Yim SCS. Simplified earthquake analysis of structures with foundation uplift. *Journal of Structural Engineering* 1985, **111**(4):906–930. https://doi.org/10.1061/(ASCE)0733-9445(1985)111:4(906).
57. Bachmann JA, Jost C, Studemann Q, Vassiliou MF, Stojadinovic B. An analytical model for the dynamic response of an elastic SDOF system fixed on top of a rocking single-story frame structure: experimental validation. ECCOMAS Congress 2016: 7th European Congress on Computational Methods in Applied Sciences and Engineering, Heraklion: 2016.
58. Hall JF, Heaton TH, Halling MW, Wald DJ. Near-source ground motion and its effects on flexible buildings. *Earthquake Spectra* 1995, **11**(4):569–605. https://doi.org/10.1193/1.1585828.
59. Makris N, Chang SP. Effect of viscous, viscoplastic and friction damping on the response of seismic isolated structures. *Earthquake Engineering and Structural Dynamics* 2000, **29**(1):85–107. https://doi.org/10.1002/(SICI)1096-9845(200001)29:1<85::AID-EQE902>3.0.CO;2-N.
60. Makris N, Vassiliou MF. The existence of 'complete similarities' in the response of seismic isolated structures subjected to pulse-like ground motions and their implications in analysis. *Earthquake Engineering and Structural Dynamics* 2011, **40**(10):1103–1121. https://doi.org/10.1002/eqe.1072.
61. Vassiliou MF, Makris N. Estimating time scales and length scales in pulselike earthquake acceleration records with wavelet analysis. *Bulletin of the Seismological Society of America* 2011, **101**(2):596–618.
62. Barenblatt GI. *Scaling, Self-Similarity, and Intermediate Asymptotics: Dimensional Analysis and Intermediate Asymptotics*, **14**. Cambridge University Press: Cambridge, UK, 1996.
63. Dimitrakopoulos EG, DeJong MJ. Revisiting the rocking block: closed-form solutions and similarity laws. *Proceedings of the Royal Society A: Mathematical, Physical and Engineering Sciences* 2012, **468**(2144): 2294–2318 https://doi.org/10.1098/rspa.2012.0026.
64. Ricker N. Further developments in the wavelet theory of seismogram structure. *Bulletin of the Seismological Society of America* 1943, **33**(3):197–228.
65. Kafle B, Lam NTK, Gad EF, Wilson J. Displacement controlled rocking behaviour of rigid objects. *Earthquake Engineering and Structural Dynamics* 2011, **40**(15):1653–1669. https://doi.org/10.1002/eqe.1107.
66. Gelagoti F, Kourkoulis R, Anastasopoulos I, Gazetas G. Rocking-isolated frame structures: margins of safety against toppling collapse and simplified design approach. *Soil Dynamics and Earthquake Engineering* 2012, **32**(1):87–102. https://doi.org/10.1016/j.soildyn.2011.08.008.
67. Drosos V, Anastasopoulos I. Shaking table testing of multidrum columns and portals. *Earthquake Engineering and Structural Dynamics* 2014, **43**(11):1703–1723. https://doi.org/10.1002/eqe.2418.
68. Ancheta TD, Darragh RB, Stewart JP, Seyhan E, Silva WJ, Chiou BSJ, et al. PEER NGA-West2 Database, PEER Report 2013/03, Pacific Earthquake Engineering Research Center. University of California, Berkeley 2013.

DOI: 10.1002/eqe